absence of this interaction (*e.g.*, for ligands not possessing such unshared pairs), the electric field gradient vanishes at the Mössbauer atom lattice point.

(C) **Isomer Shift.**—The isomer shifts with respect to SnO_2 which are observed in this study are also summarized in Table I and are seen to be similar to those reported[27] for other organotin compounds. Closer examination shows that the isomer shifts for the hydrides fall into two distinct groups. One group shows a shift of 1.24 ± 0.03 mm sec^{-1}, while the other group shows a shift of 1.42 ± 0.04 mm sec^{-1}. This grouping effect is clearly outside of experimental error and is also evident from the data of Aleksandrov, *et al.*[22] The presently available data show that organotin compounds of the type R_nSnH_{4-n} (R is either an alkyl or aryl group) in which there is at least one CH_3–Sn bond will have isomer shifts which are ~0.18 mm sec^{-1} more negative than the shifts for organotin compounds with no methyl–tin bonds. This distinctive behavior of methyl–tin compounds is clearly not due primarily to steric factors, since such factors would be noted in the Mössbauer parameters for the systematic replacement series *i*-C_3H_7, *n*-C_4H_9, *i*-C_4H_9, C_6H_5. That such steric effects are absent is clearly seen from the data in Table I and ref 22.

Finally, it is evident from these data that the observed isomer shift for SnH_4 is considerably smaller than that which would have been predicted from simple electronegativity considerations. The correlations suggested earlier[2,31] for isomer shifts of SnA_4 molecules give a value for SnH_4 which is approximately 0 4 mm sec^{-1} larger than the value observed experimentally. A detailed examination of the relationship between ligand electronegativity, bond character, and steric parameters of organotin compounds and their corresponding Mössbauer parameters is currently under way in these laboratories.

Acknowledgment.—The authors are indebted to Professor S. Shupack and Mr. H. A. Stöckler for a number of enlightening discussions of this work. This research was supported in part by the U. S. Atomic Energy Commission and the Petroleum Research Fund of the American Chemical Society, and this support is hereby gratefully acknowledged.

(31) V. I. Goldanskii, "The Mössbauer Effect and Its Applications in Chemistry," Consultants Bureau, New York, N. Y., 1964.

CONTRIBUTION FROM THE CHEMISTRY DIVISION, DEPARTMENT OF SCIENTIFIC AND INDUSTRIAL RESEARCH, WELLINGTON, NEW ZEALAND, AND CHEMISTRY DEPARTMENT, VICTORIA UNIVERSITY OF WELLINGTON, WELLINGTON, NEW ZEALAND

Magnetic Susceptibility and Mössbauer Results of Some High-Spin Iron(II) Compounds[1a]

BY R. M. GOLDING,[1b] K. F. MOK,[1c] AND J. F. DUNCAN[1c]

Received September 30, 1965

Using iron(II)–pyridine complexes as examples, we have explored the relation between the average magnetic moments, μ, and the Mössbauer parameter, ΔE_Q, assuming that the iron nucleus is in an environment of tetragonal symmetry—a distortion from octahedral symmetry. ΔE_Q is very sensitive to small deviations from octahedral symmetry whereas the average magnetic moment is insensitive.

Introduction

The applications of the Mössbauer effect to the study of chemical compounds has led to an investigation of the physical meaning of the parameters ΔE_Q (quadrupole splitting) and the isomer shift. A general theoretical treatment of the problem[2] has revealed that ΔE_Q and magnetic moment, μ, are directly related, and both can be used for investigating the asymmetry of the environment of the iron nucleus.

The treatment for low-spin iron(III) compounds is discussed elsewhere.[2] Here we are concerned solely with high-spin iron(II) compounds, and we have used results obtained for a series of pyridine derivatives as illustrated examples.

Experimental Section

The methods by which the pyridine compounds were prepared were as follows.

(i) **$Fe(py)_4Cl_2$.**—Pure iron powder (5 g) was gradually added to 15 ml of AnalaR concentrated hydrochloric acid. When the hydrogen had ceased to evolve, about 20 ml of methanol was added and the solution was filtered into a flask containing 100 ml of pyridine under a nitrogen atmosphere. Intense yellow crystals separated out immediately. The mixture in the flask was allowed to stand overnight in the inert gas atmosphere. The crystals were filtered off and recrystallized from pyridine and were filtered and dried in a vacuum desiccator. *Anal.* Calcd for $Fe(py)_4Cl_2$: Fe, 12.6; C, 54.2. Found: Fe, 12.6; C, 53.4.

(ii) **$Fe(py)_4Br_2$.**—This was prepared according to the method of Weinland, *et al.*[3] Bromine (1.5 ml) was slowly added to 3 g of pure iron powder in 20 ml of methanol. When the reaction had ended, the solution was filtered with stirring into a flask containing 50 ml of pyridine. The mixture was allowed to

(1) (a) This work was partially supported by U.S.A.F. Grant No. 27–63; (b) Department of Scientific and Industrial Research; (c) Victoria University of Wellington.

(2) R. M. Golding, to be published.

(3) R. Weinland, K. Effinger, and V. Beck, *Arch. Pharm.*, **265**, 352 (1927).

stand for a few hours in a nitrogen atmosphere when the yellow crystals were filtered and dried in a vacuum desiccator. The complex was recrystallized from pyridine. *Anal.* Calcd for $Fe(py)_4Br_2$: Fe, 10.5; C, 45.1. Found: Fe, 9.9; C, 46.3.

(iii) **$Fe(py)_4I_2$.**—Finely divided iodine (7 g) was gradually added to 2 g of pure iron powder in 20 ml of methanol. The solution was filtered with stirring into a flask containing 50 ml of pyridine. The mixture was allowed to stand for a few hours in a nitrogen atmosphere. The crystals were filtered and dried in a vacuum desiccator and then recrystallized from methanol. *Anal.* Calcd for $Fe(py)_4I_2$: Fe, 8.9; C, 38.4; I, 40.55. Found: Fe, 8.9; C, 38.0; I, 39.3.

(iv) **$Fe(py)_4I_2 \cdot 2py$.**—This was prepared in the same way as the tetrapyridine iodide except that it was finally recrystallized from pyridine only. *Anal.* Calcd for $Fe(py)_4I_2 \cdot 2py$: Fe, 7.1; C, 45.9; I, 32.4. Found: Fe, 7.2; C, 45.4; I, 31.8.

(v) **$Fe(py)_4(SCN)_2$.**—This was prepared according to the method of Spacu and Armeanu.[4] Iron(II) sulfate heptahydrate (4.4 g) in a small amount of distilled water was added to 3.1 g of potassium thiocyanate in a small amount of water. About 50 ml of pyridine was then added to the syrupy liquid. The yellow crystals of the complex separated out and were filtered off. The crude product was then recrystallized from pyridine. The crystals were dried in a vacuum desiccator. *Anal.* Calcd for $Fe(py)_4(SCN)_2$: Fe, 11.4; C, 54.1. Found: Fe, 11.3, C, 54.4.

(vi) **$Fe(py)_4(OCN)_2$.**—This was prepared in a similar way to the thiocyanate. Iron(II) sulfate heptahydrate (2.78 g) and 1.62 g of potassium cyanate were used. The crude product was recrystallized from methanol and dried in a vacuum desiccator. *Anal.* Calcd for $Fe(py)_4(OCN)_2$: Fe, 12.3; C, 57.9. Found: Fe, 12.4; C, 57.5.

(vii) **$Fe(py)_4(OCN)_2 \cdot 2py$.**—This was prepared by the same method as the tetrapyridine cyanate complex except that the compound was recrystallized from pyridine only. *Anal.* Calcd for $Fe(py)_4(OCN)_2 \cdot 2py$: Fe, 9.1; C, 62.5. Found: Fe, 9.0; C, 60.5.

The Mössbauer measurements for finely powdered samples (20 mg of iron/cm^2) of the iron complexes were obtained at room temperature with a standard Mössbauer spectrometer built around an R.I.D.L. 400-channel analyzer used in time mode. The velocity modulation was achieved by a transducer vibrated sinusoidally at 30 c/sec. The spectrometer was calibrated with potassium nitroprusside powder and 0.001 in. thick iron foil. Visual graphing was used to obtain the data from the Mössbauer spectra, the errors estimated as ±0.10 mm/sec.

Results and Discussion

In the series of compounds chosen ($Fe(py)_4X_2$, where py = pyridine, X^- = Cl^-, Br^-, I^-, SCN^-, and OCN^-), the extent of deviation from octahedral symmetry of the environment of the iron atom would be expected to vary with the nature of X^-. This in turn is reflected in the changes in the Mössbauer spectra, ultraviolet spectra, and the magnetic moments. The quadrupole splittings, the isomer shifts, and the magnetic moments were measured at room temperature for ten compounds, the results being summarized in Table I. We interpret the variations of the Mössbauer and magnetic data in the series of iron–pyridine (and iron–phenanthroline) complexes as arising from varying degrees of pseudo-axial distortion of the environment of the iron atom from the crystal field of octahedral symmetry.

Theoretical Considerations.—The magnetic susceptibility of a regular octahedral complex is isotropic. However, many octahedral transition metal ion complexes yield magnetic anisotropies of up to 30%.[5,6] Van Vleck[7] attributed this anisotropy to at least a partial removal of the ground-state degeneracy. In this section we calculate the magnetic susceptibility, χ, and the quadrupole splitting, ΔE_Q, of the high-spin iron(II) atom in a pseudo-axial field.

TABLE I

THE MÖSSBAUER AND MAGNETIC MOMENT RESULTS AT ROOM TEMPERATURE

Compd[a]	ΔE_Q (±0.10), mm/sec	Isomer shift[b] (±0.10), mm/sec	μ, BM
(a) $Fe(py)_4Cl_2$	3.14	1.13	5.34
(b) $Fe(py)_4Br_2$	2.52	1.16	5.28
(c) $Fe(py)_4I_2$	0.65	1.25	5.90
(d) $Fe(py)_4I_2 \cdot 2py$	0.83	1.17	5.64
(e) $Fe(py)_4(SCN)_2$	1.52	1.21	5.47
(f) $Fe(py)_4(OCN)_2$	2.52	1.24	5.13
(g) $Fe(py)_4(OCN)_2 \cdot 2py$	2.59	1.24	5.20
(h) $Fe(phen)_2Cl_2$	3.28	1.15	5.27[c]
(i) $Fe(phen)_2Br_2$	3.26	1.16	5.15[c]
(j) $Fe(phen)_2(SCN)_2$	3.09	1.13	5.22[c]

[a] py = pyridine; phen = 1,10-phenanthroline. [b] Reference stainless steel. [c] B. Bleaney and K. W. H. Stevens, *Rept. Progr. Phys.*, **16**, 108 (1953).

(i) **Magnetic Susceptibility, χ.**—We start by considering the octahedral crystal field case with a $^5T_2$ ground state (the weak field case for the d^6 iron) with excited states sufficiently high in energy for spin–orbit mixing into the ground state to be neglected. The degeneracy of the $^5T_2$ state will be partially lifted by any perturbation distorting the octahedral crystal field to a resulting field of trigonal or tetragonal symmetry yielding two states. However, in general, a rhombic field will completely lift the orbital degeneracy yielding three states, the separation of the states depending on the degree of distortion from octahedral symmetry. In order to compare the magnetic moment and the quadrupole splitting of an iron(II) compound in a rhombic crystal field would require a detailed study of each compound investigated with the estimation of several parameters from the experimental data. However, to gain an understanding of the relationship between magnetic susceptibility and Mössbauer results in a series of iron(II) complexes we shall follow Van Vleck[7] and consider the iron atom in a crystal field of tetragonal symmetry. The separation between the two states, Δ, depends on the explicit model chosen for the molecule, and normally for ferrous compounds the ground state is orbitally nondegenerate.[7-9] Therefore, we shall first consider the result of a crystal field distortion of tetragonal symmetry, the ground state becoming nondegenerate and the first excited state double degenerate. This distortion may be represented[10] by the operator $\sum_i (\Delta/3) l_{iz}^2$.

The spin–orbit coupling interaction $\sum_i \zeta l_i \cdot s_i$ and the

(4) G. Spacu and V. Armeanu, *Bul. Soc. Stiinte Cluj*, **7**, 566 (1934).

(5) I. I. Rabi, *Phys. Rev.*, **29**, 174 (1927).

(6) K. S. Krishnan, A. Mookherji, and A. Bose, *Phil. Trans. Roy. Soc. London*, **A238**, 125 (1939).

(7) J. H. Van Vleck, *Discussions Faraday Soc.*, **26**, 96 (1958).

(8) R. Ingalls, *Phys. Rev.*, **A133**, 787 (1964).

(9) D. Palumbo, *Nuovo Cimento*, **8**, 271 (1958).

(10) J. S. Griffith, "The Theory of Transition-Metal Ions," Cambridge University Press, Cambridge, 1961.

magnetic field interaction $\sum_i \beta(l_i + 2s_i)\cdot H$ are next considered. These interactions may be represented by the Hamiltonian

$$\mathcal{H} = \sum_i \left\{ \frac{\Delta}{3} l_{iz}^2 + \zeta l_i \cdot s_i + \beta(l_i + 2s_i)\cdot H \right\}$$

The calculations are facilitated by the isomorphic property of the p and d electrons[10] whereby we may consider the $^5T_2$ term as equivalent to ^5P_J; here J = 3, 2, 1. For our particular case this leads to a change in the Hamiltonian which now becomes

$$\mathcal{H} = \sum_i \left\{ \delta\left(l_{iz}^2 - \frac{2}{3} \right) + \frac{\xi}{4} l_i \cdot s_i + \beta(-l_i + 2s_i)\cdot H \right\}$$

The factor $^2/_3$ is introduced so that the center of gravity of the energy levels is unaffected since we require only the relative order of the energy levels; δ ($= \Delta/3$) is positive if the nondegenerate state is the ground state.

We choose $\phi(JM)$, the basic set of wave functions, as

$$\phi(JM) = \sum_{M_L M_S} \langle 1\ 2\ M_L M_S | 1\ 2 JM \rangle | M_L M_S \rangle$$

since the matrix is then diagonalized with respect to the spin–orbit coupling interaction. $\langle 1\ 2\ M_L M_S | 1\ 2\ JM \rangle$ are Clebsch–Gordon–Wigner coefficients and $|M_L M_S\rangle$ are p-like atomic orbitals in the $M_L M_S$ notation. We consider the magnetic field in the xz plane at an angle θ to the z direction. We were unable to solve this matrix for the general case and therefore proceeded by first diagonalizing for various ratios of δ/ζ and then treating the magnetic field interaction as a small perturbation.

From the 15 eigenvalues, E_n, so obtained, the magnetic susceptibility was calculated in the usual manner where

$$\chi = \frac{N}{H} \frac{\sum_n (-\partial E_n/\partial H) \exp(-E_n/kT)}{\sum_n \exp(-E_n/kT)}$$

The magnetic susceptibility can be written in the form

$$\chi = \chi_\parallel \cos^2\theta + \chi_\perp \sin^2\theta$$

where $\chi_\parallel$ is the magnetic susceptibility when the magnetic field is parallel to the z direction (the distortion axis) and $\chi_\perp$ is obtained when the magnetic field is in the xy plane. The magnetic moment, μ, is defined as

$$\chi = N\beta^2\mu^2/3kT$$

and the definitions of $\mu_\parallel$ and $\mu_\perp$ follow. The average magnetic moment, μ, is given by the relationship

$$\mu^2 = \frac{1}{3}(\mu_\parallel^2 + 2\mu_\perp^2)$$

The calculated results may be written in the form

$$\mu^2 = \frac{\sum_{n=1}^{9} (A_n + B_n/x) \exp(a_n x)}{\sum_{n=1}^{6} 2 \exp(a_n x) + \sum_{n=7}^{9} \exp(a_n x)} \qquad (1)$$

TABLE II

THE A_n, B_n, AND C_n PARAMETERS FOR VARIOUS VALUES OF δ/ζ

n	a_n	$\mu_\parallel^2$ A_n	$\mu_\parallel^2$ B_n	$\mu_\perp^2$ A_n	$\mu_\perp^2$ B_n	C_n
			$\delta/\zeta = 0.5$			
1	−0.6667	54.0000	0	0	−300.0120	+1.0000
2	−0.5571	11.9049	−12.3204	0	−158.9688	0.5914
3	0.4738	77.3889	12.3204	0	−148.7668	−1.5914
4	−0.4610	0.3636	−60.8796	0	−340.9824	+0.1078
5	0.1637	58.2903	−4.7688	0	477.1404	+0.5752
6	0.7973	41.7258	65.6484	0	−2270.3484	−0.6836
7	−0.4167	0	− 64.7724	0	693.3315	−0.0999
8	0.0833	0	35.9682	0	−438.0573	+0.5000
9	0.8333	0	28.8042	0	2486.6649	−0.4001
			$\delta/\zeta = 1.0$			
1	−0.8333	54.0000	0	0	−246.0732	+1.0000
2	−0.6764	8.5611	−4.5552	0	−100.4052	+0.8056
3	0.7597	86.9139	4.5552	0	−293.6496	−1.8056
4	−0.5200	0.5748	44.4900	0	−70.4760	+0.5488
5	0.0529	101.6586	18.8556	0	286.1076	+0.7482
6	0.9670	28.8714	25.6344	0	−1855.7892	−1.2972
7	−0.4264	0	−119.8110	0	301.3452	+0.1418
8	−0.0833	0	108.0084	0	−195.1344	+0.5000
9	1.0097	0	11.8026	0	2174.0748	−0.6419
			$\delta/\zeta = 2.0$			
1	−1.1667	54.0000	0	0	−218.8333	+1.0000
2	−0.9708	6.8568	−1.0290	0	−87.9712	+0.9310
3	1.3876	92.7156	1.0290	0	−541.7248	−1.9310
4	−0.7658	3.3816	−18.3221	0	0.2758	+0.8532
5	−0.2294	134.6168	13.7742	0	203.7685	+0.9112
6	1.4952	24.3410	4.5479	0	−2258.6975	−1.7644
7	−0.6096	0	−254.4268	0	163.5173	+0.3645
8	−0.4166	0	251.9139	0	−73.5869	+0.5000
9	1.5264	0	2.5129	0	2813.2520	−0.8645
			$\delta/\zeta = 2.5$			
1	−1.3333	54.0000	0	0	−213.5664	+1.0000
2	−1.1280	6.5805	−0.5897	0	−87.8231	+0.9526
3	1.7115	93.7421	0.5897	0	−664.9682	−1.9526
4	−0.9128	4.1559	−12.5569	0	6.1908	+0.9040
5	−0.3840	140.0227	10.1758	0	192.9865	+0.9408
6	1.7968	24.0314	2.3812	0	−2646.2561	−1.8446
7	−0.7393	0	−325.0026	0	140.7523	+0.4087
8	−0.5833	0	323.6354	0	−49.2456	+0.5000
9	1.8225	0	1.3672	0	3321.9298	−0.9088

where $x = \zeta/kT$. The parameters A_n, B_n, and a_n are given in Table II for δ/ζ = 0.5, 1.0, 2.0, and 2.5. The magnetic moment, therefore depends on three variables: T, the absolute temperature; ζ, the spin–orbit coupling constant; and δ, the distortion parameter. The effect of the distortion parameter on the magnetic moments is illustrated in Figures 1 and 2.

(ii) **Quadrupole Splitting, ΔE_Q.**—For d electrons the nuclear–quadrupole moment interaction may be represented[11] by the Hamiltonian

$$\mathcal{H}' = \frac{e^2 Q' \langle r^{-3} \rangle}{7I(2I-1)} \sum_i \left\{ (l_i \cdot I)^2 + \frac{1}{2}(l_i \cdot I) - 2I(I+1) \right\}$$

where I is the nuclear spin, Q' is the quadrupole moment (including any shielding effects), and r is the radius of the d electron. The Hamiltonian we now need to consider is

$$\mathcal{H} = \sum_i \left\{ \delta\left(l_{iz}^2 - \frac{2}{3} \right) + \frac{\zeta}{4} l_i \cdot s_i \right\} + \mathcal{H}'$$

In section i we have already diagonalized the distortion and spin–orbit coupling interaction matrix for various δ/ζ ratios and we shall use these eigenfunctions,

(11) See footnote *c* of Table I.

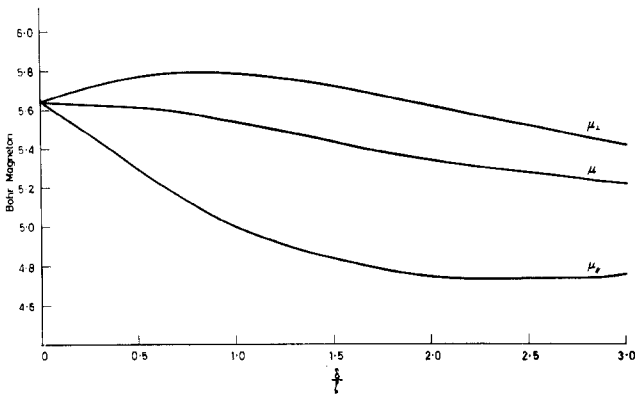

Figure 1.—A plot of $\mu_{||}$, $\mu_{\perp}$, and μ against δ/ζ when $\zeta/kT = 2$ to illustrate the dependence of the magnetic moments on the distortion parameter δ.

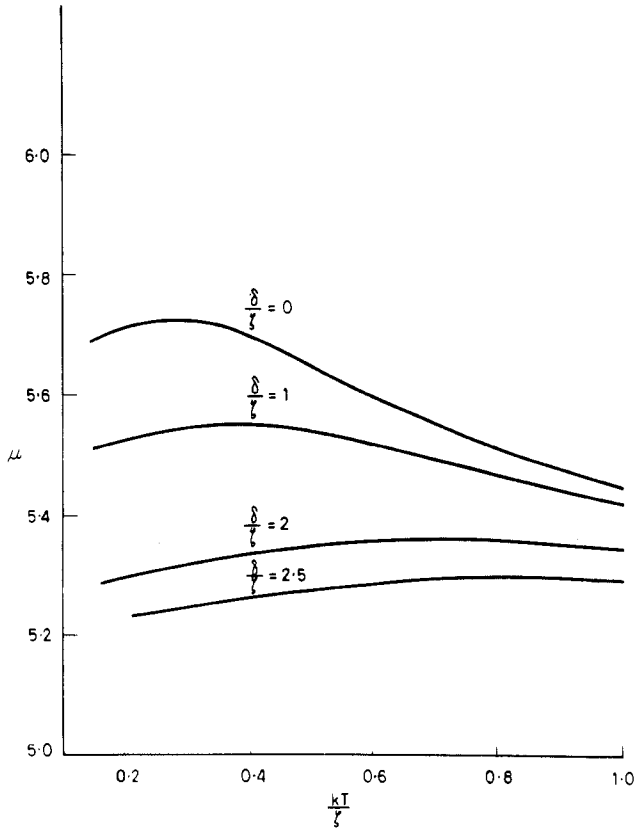

Figure 2.—A plot of the average magnetic moment, μ, against kT/ζ for $\delta/\zeta = 0$, 1.0, 2.0, and 2.5.

Ψ_n, as our basic set. Since $\mathcal{H}'$ is a very small perturbation, we may consider only the diagonal matrix elements, $\langle\Psi_n|\mathcal{H}'|\Psi_n\rangle$. Hence, E_{nQ}, the nuclear–quadrupole moment interaction energy, is

$$E_{nQ} = \langle\Psi_n M_I|\mathcal{H}'|\Psi_n M_I\rangle = \frac{e^2Q'\langle r^{-3}\rangle}{14I(2I-1)}\{3M_I^2 - I(I+1)\}C_n$$

where C_n is given in Table II.

The average E_Q values, $\langle E_Q\rangle$, follow[12]

$$\langle E_Q\rangle = \frac{e^2Q'\langle r^{-3}\rangle}{14I(2I-1)}\{3M_I^2 - I(I+1)\}\frac{\sum_n C_n \exp(a_n x)}{\sum_n \exp(a_n x)}$$

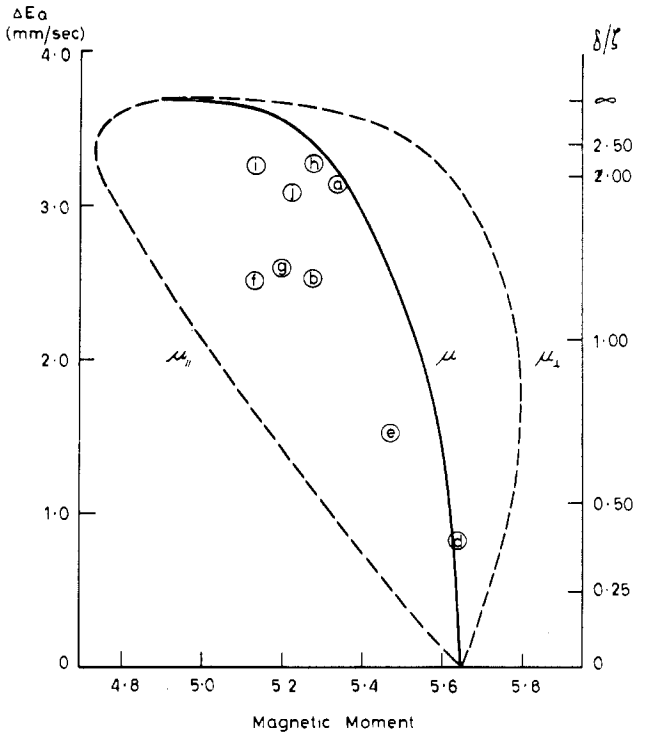

Figure 3.—The relationship among ΔE_Q, the magnetic moment, and the distortion parameter for high-spin ferrous compounds. The theoretical curves are plotted for the case when $\zeta/kT = 2$. The experimental points refer to the compounds in Table I.

For the ^{57}Fe nucleus, $I = {}^3/_2$ in the excited state and the quadrupole splitting is the difference between the nuclear states $M_I = \pm{}^1/_2$ and $M_I = {}^3/_2$. Therefore

$$\Delta E_Q = \langle E_Q\rangle(M_I = \pm{}^3/_2) - \langle E_Q\rangle(M_I = \pm{}^1/_2) = \frac{1}{7}e^2Q'\langle r^{-3}\rangle\frac{\sum_n C_n(\exp(a_n x)}{\sum_n(\exp(a_n x)} = 1.85\frac{\sum_n C_n \exp(a_n x)}{\sum_n \exp(a_n x)} \quad \text{(mm/sec)} \qquad (2)$$

(See ref 2 for a discussion of the numerical constant.)

(iii) **Relation between ΔE_Q and μ.**—Using eq 1 and 2 we may relate ΔE_Q and μ for various ratios of δ/ζ. This plot is shown as the solid line in Figure 3. (The curves for $\mu_{||}$ and $\mu_{\perp}$ are also indicated.) ΔE_Q is very sensitive to small distortions from octahedral symmetry whereas this is not the case for the average magnetic moment.

Interpretation of Experimental ΔE_Q and μ Values.—The observed ΔE_Q and μ values at room temperature for the iron–pyridine and iron–phenanthroline series are quoted in Table I. ΔE_Q and μ are related: when μ is large, ΔE_Q is small. The experimental results are plotted in Figure 3, and there is satisfactory agreement with the theoretical curve ($\zeta/kT = 2$); no bonding effects have been considered.

Interpretation of Previously Published Magnetic Moment Values.—From the ΔE_Q value at room tem-

(12) This treatment parallels ref 8 presenting the data in a different form.

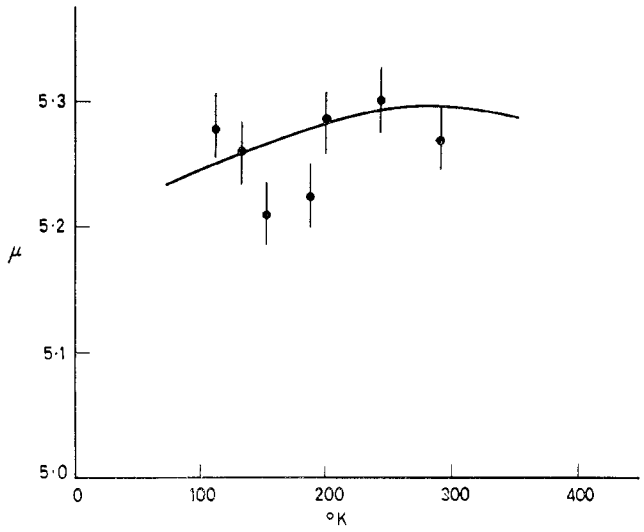

Figure 4.—A plot of magnetic moment, μ, against temperature for $Fe(phen)_2Cl_2$. The solid line is our calculated curve choosing the spin–orbit coupling constant, ζ, as 250 cm^{-1} and the distortion parameter, δ, as 625 cm^{-1}. The points are the experimental results from ref 13; we have indicated the minimum error likely in the magnetic moment measurements.

perature for $Fe(phen)_2Cl_2$, $\delta/\zeta \sim 2$ (see Figure 3), yielding about 800 cm^{-1} for the parameter δ. The average magnetic moment for this and other iron–phenanthroline complexes over a wide range of temperature has recently been measured.[13] At room temperature the powders give magnetic moments between 5.1 and 5.3 BM, and the temperature dependence of the moments shows a slight maximum at about 250°K. The temperature variation predicted by eq 1 may be fitted to the experimental results as shown in Figure 4 on which we have indicated the minimum error in μ usually expected due to packing of the material[14]—the absolute experimental error may be greater (compare results in ref 13 and 15). The solid line in Figure 4 is our calculated curve obtained by choosing $\mu_{max} = 5.29$ at 250°K. This yields a spin–orbit coupling constant of 250 cm^{-1} and a distortion δ of 625 cm^{-1} ($\delta/\zeta = 2.5$)—see Figure 2 to choose the appropriate δ/ζ curve. The calculated value for the spin–orbit coupling constant is less than the value for the Fe^{2+} free ion of 400 cm^{-1}.[10] However, this difference may be explained by strong bonding of the metal ion d orbitals with the ligand orbitals, for we have assumed in our calculations that there is no mixing of the metal ion d orbitals with the ligand orbitals. Mössbauer and magnetic moment measurements both indicate that the separation of the ground state arising from a pseudo-axial field is about 2000 cm^{-1} (3δ) which confirms the conclusions drawn from the ultraviolet absorption spectra of these complexes.[15]

Finally, we shall reconsider the assumptions in choosing the model proposed to explain the experimental results of these compounds in the light of the theoretical treatments. If the orbitally nondegenerate state is the ground state, we have shown that ΔE_Q (as defined in eq 2) is positive and the maximum value is +3.7 mm/sec, but, if the orbitally degenerate state is the ground state, ΔE_Q is negative and the minimum value is −1.9 mm/sec. Thus, the sign of the quadrupole splitting from the experimental results would readily confirm the ground state. However, to determine experimentally the sign of the quadrupole splitting,[16] we require a single crystal of known structure. Unfortunately, such information is at present not available for these series of iron compounds. However, the magnitude of most of the quadrupole splittings of these compounds studied are greater than 2 mm/sec (Table I). This, therefore, supports the assumption that the ground state is most likely the orbitally nondegenerate state.

A general consideration of the bonding of the d electrons with the ligands would lead to a very complex expression for the electric field gradient at the iron nucleus with further unknown parameters due to asymmetric bonding. To gain at least a partial understanding of the bonding, we have assumed symmetric bonding, the degree of bonding being reflected in the experimental values of the spin–orbit coupling constant.

As has been shown, information can be gained about the environment of the iron atom in these compounds from one measurement by considering a one-unknown-parameter (the δ/ζ ratio) model. If the average magnetic moment and the quadrupole splitting were accurately known at one temperature for a compound, then both δ and ζ could be estimated from eq 1 and 2. Unfortunately, the normal experimental error in magnetic susceptibility measurements is too great for a detailed analysis in this way. However, as illustrated above, a temperature-dependent study of the experimental results of these compounds would yield further information about the δ and ζ values. To determine the exact form of the distortion from octahedral symmetry would require a detailed magnetic susceptibility study of single crystals of these complexes to elucidate the three principal magnetic moment values. Without this information we have assumed the simpler model.

Conclusions

The quadrupole splittings of the iron–pyridine and iron–phenanthroline complexes have been explained on the assumption that the iron atom is in a pseudo-axial crystal field. This model has enabled the variation in ΔE_Q and in the magnetic moments and the observed ΔE_Q relationship of these complexes to be interpreted. Hence, from the quadrupole splitting of high-spin d^6 iron complexes and from Figure 3, not only can the average magnetic moment be predicted but the splitting of the $^5T_2$ ground state can readily be ascertained.

(13) W. A. Baker and H. M. Bobonich, *Inorg. Chem.*, **3**, 1184 (1964).
(14) B. N. Figgis and J. Lewis, "Modern Coordination Chemistry," Interscience Publishers, Inc., New York, N. Y., 1960, Chapter 6.
(15) K. Madeja and E. König, *J. Inorg. Nucl. Chem.*, **25**, 377 (1963).
(16) J. F. Duncan and R. M. Golding, *Quart Rev.* (London), **14**, 36 (1965).